

INSTRUCTIONS TO PREPARE A FULL PAPER FOR THE 9TH EUROPEAN CONGRESS ON COMPUTATIONAL METHODS IN APPLIED SCIENCES AND ENGINEERING ECCOMAS CONGRESS 2024

FIRST A. AUTHOR¹, SECOND B. AUTHOR² AND THIRD C. AUTHOR¹

¹ International Center for Numerical Methods in Engineering (CIMNE)
Universidad Politécnica de Cataluña
Campus Norte UPC, 08034 Barcelona, Spain
e-mail: congress@cimne.upc.edu, www.cimne.com

² Spanish Association for Numerical Methods in Engineering (SEMNI)
Edificio C1, Campus Norte UPC
Gran Capitán s/n, 08034 Barcelona, Spain
email: semni@cimne.upc.edu, www.semni.org

Key words: Computational Mechanics, FEM, Contact Problems

Summary. This document provides information and instructions for preparing a Full Paper to be included in the Proceedings of *ECCOMAS CONGRESS 2024*.

1 INTRODUCTION

orig: 10.95\normalsize 10.95It seems that the font size is actually set to 11pt, although 12pt should be used in the body of the text.

All the participants whose Abstract has been accepted for presentation at the ECCOMAS 2022 Congress are kindly requested to submit the Full Paper electronically via the web page of the Congress, before **July 1st, 2024**. Congress Proceedings (including full papers only) will be published on Scipedia with DOI number after the congress and will be submitted for indexation to SCOPUS database. Submission of the full paper is not mandatory. The Full Paper should be written following the format of macros for submission. The file has to be translated into Portable Document Format (PDF) before submission via the Conference site. The organizers do not commit themselves to include in the Proceedings any Full Paper received later than the above-mentioned deadline. The corresponding author should be the speaker, and is expected to register and pay his registration fee during the advance period (before **April 1st, 2024**) for the paper to be included in the technical programme of the ECCOMAS 2024.

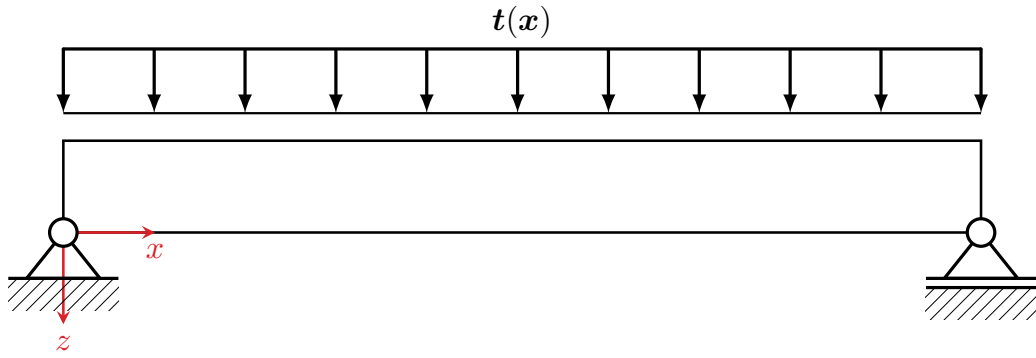


Figure 1: Schematic representation of the structural problem. A simply supported beam is subjected to a constant load.

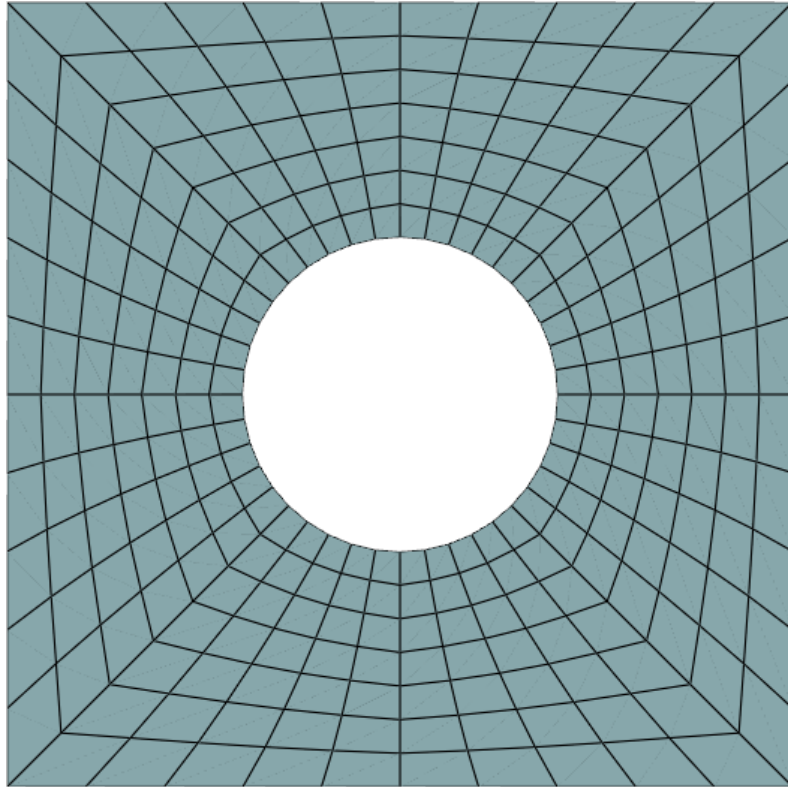


Figure 2: Unit cell domain partition.

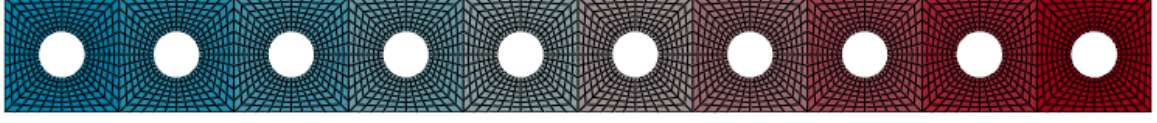


Figure 3: The partition of the global domain. The colors indicate the variation in Young's modulus for each subdomain.

Table 1: HAPOD inner

Edge	Basis size	Snapshots	Average basis size after RRF
bottom	23	605	10
left	38	686	11
right	38	681	11
top	24	604	10

2 METHODS

3 RESULTS

3.1 Problem setup

3.2 Basis Construction

For the beam problem, there are three oversampling problems to consider (left, inner, right). For each of the associated parametric transfer operators, n_{train} parameter samples are chosen, and the range for each of these (fixed) transfer operators is approximated via random sampling. In the sampling *normal* or *multivariate normal* distribution is used. The range approximation of the n_{train} transfer operators yields n_{train} sets of basis functions, which are further compressed via POD, to obtain the final parameter independent basis functions (POD modes).

Table 2: Heuristic rrf inner

Edge	Basis size	Basis size after RRF	Neumann modes
bottom	30	19	11
left	38	25	13
right	38	25	13
top	27	17	10

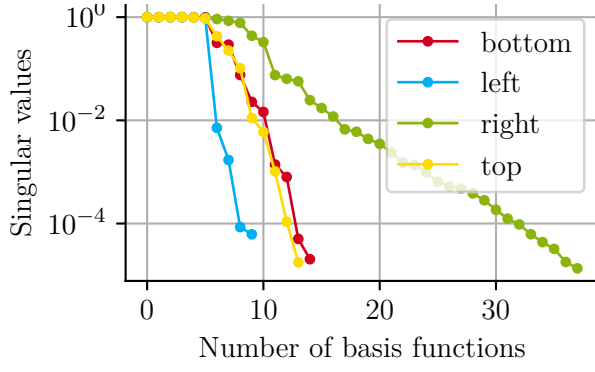


Figure 4: Singular value left

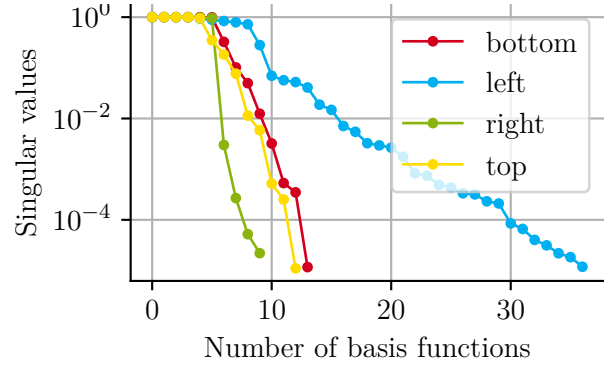


Figure 5: Singular value right

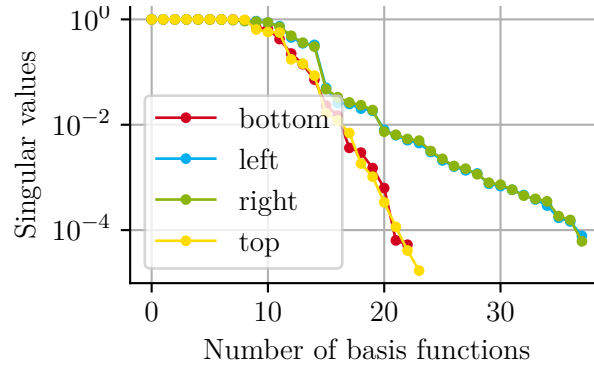


Figure 6: Singular value inner

3.2.1 Distributed approximate POD

3.2.2 Heuristic range finder

3.3 Localized ROM

3.4 Optimization problem

4 FORMAT OF REFERENCES

References should be quoted in the text by superscript numbers [1, 2, 3] and grouped together at the end of the Full Paper in numerical order as shown in these instructions.

Table 3: Result of the optimization with FOM and ROM.

Model	Iterations	Evaluations	Time	Output J
	-	-	s	N mm
FOM	5	99	16.867	51.559
ROM	5	99	0.188	51.559

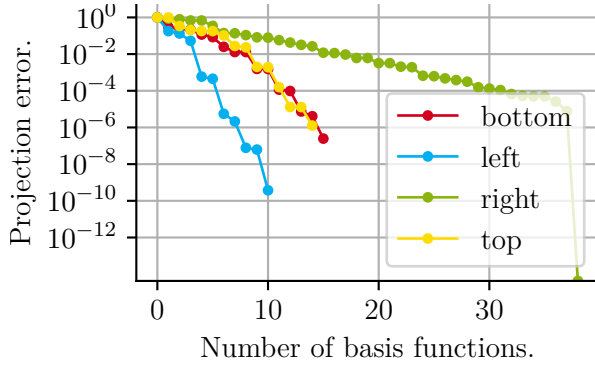


Figure 7: Projection error hapod

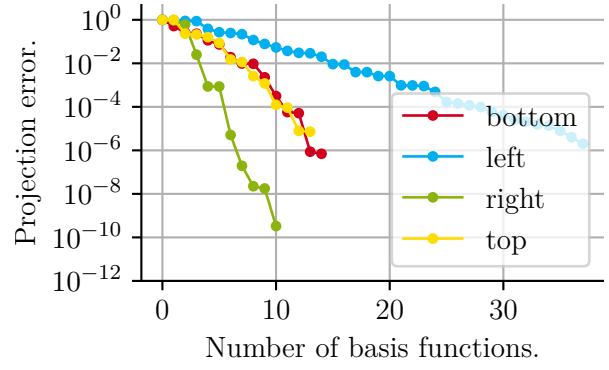


Figure 8: Projection error hapod

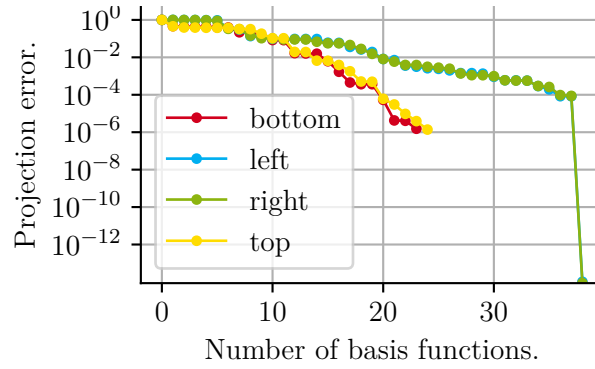


Figure 9: Projection error hapod

5 CONCLUSIONS

- Full Papers in format for publication should be submitted electronically via the web page of the Conference, before **July 1st, 2024**. They must be converted to Portable Document Format (PDF) before submission. The maximum size of the file is 4 Mb.

REFERENCES

- [1] McQuerry, M. 2018. "Validation of a Clothing Heat Transfer Model in Non-isothermal Test Conditions." J Test Eval 46, no. 1 (January/February): 1–7. <http://doi.org/10.1520/JTE20170073>
- [2] National Stone, Sand, and Gravel Association (NSSGA). 2013. The Aggregates Handbook, 2nd ed. Englewood, CO: Society of Mining, Metallurgy, and Exploration.
- [3] Oden, C. P., C. L. Ho, and H. F. Kashani. 2018. "Man-Portable Real-Time Ballast Inspection Device Using Ground-Penetrating Radar." In Railroad Ballast Testing and Properties, edited by T. Stark, R. Swan, and R. Szczy, 77–104. West Conshohocken, PA: ASTM International. <http://doi.org/10.1520/STP160520170023>

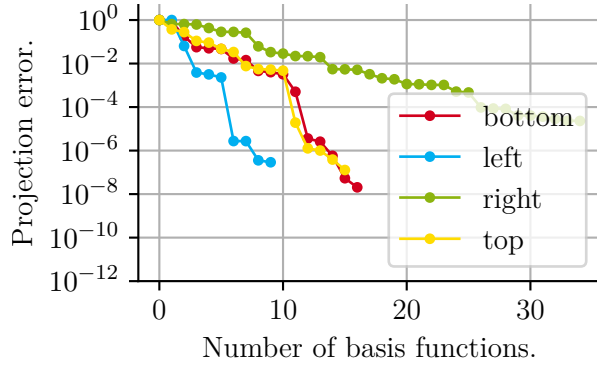


Figure 10: Projection error

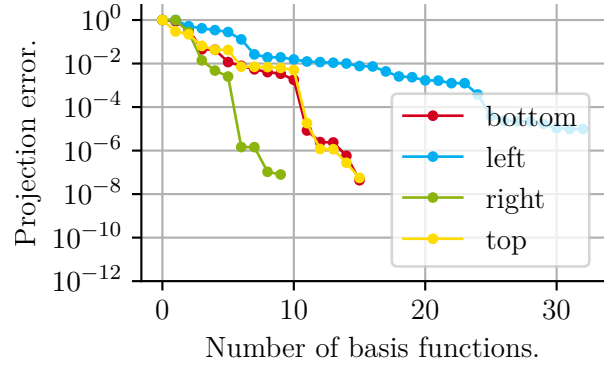


Figure 11: Projection error

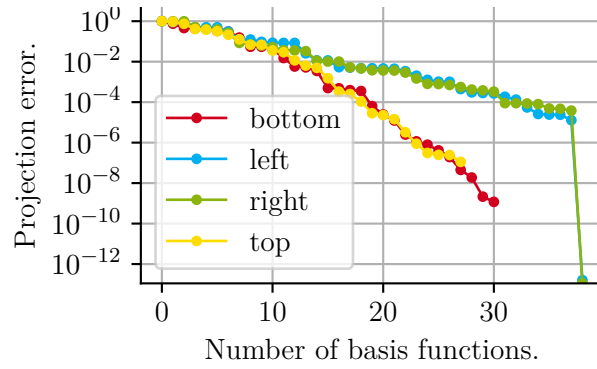


Figure 12: Projection error

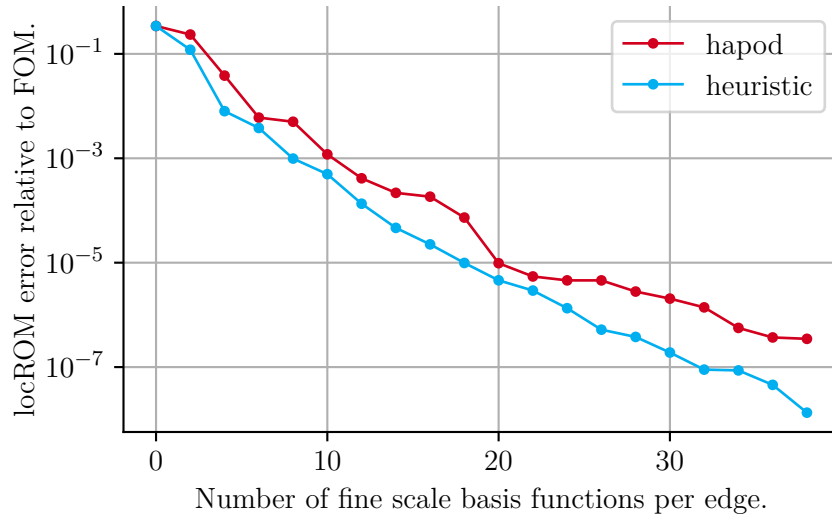


Figure 13: Local ROM error relative to FOM.

Table 4: Comparison of reduced optimal solution μ_N^* and true optimal solution μ^* .

Beam example		
True output	$J(\mu^*)$	51.5594
Reduced output	$J_N(\mu_N^*)$	51.5591
True output at μ_N^*	$J(\mu_N^*)$	51.5592
Abs. error in optimal solution	$\ \mu_N^* - \mu^*\ $	0.0129
Abs. error in output	$ J_N(\mu_N^*) - J(\mu^*) $	$2.2605 \cdot 10^{-4}$
Suboptimality	$\frac{J(\mu_N^*) - J(\mu^*)}{J(\mu^*)}$	$3.3261 \cdot 10^{-6}$